Journal of Ambient Intelligence and Humanized Computing
https://doi.org/10.1007/s12652-020-02812-3

ORIGINAL RESEARCH

Intelligent charging control method of shared vehicle based on MPPT algorithm in the environment of internet of things

Ling Ma[1] · **Ye'an Lu**[2]

Received: 23 June 2020 / Accepted: 9 December 2020

Abstract
With the gradual popularization of shared vehicles, the large-scale access of electric vehicle charging pile will have a significant impact on the operation planning of power grid. Therefore, a vehicle charging control strategy based on the Internet of things is proposed. Combined with the basic principle of MPPT algorithm and fully considering the actual needs, the peak load of the charging pile is adjusted from the load limit, and the voltage energy consumption of the charging circuit is accurately controlled to realize the intelligent charging of the shared vehicle. The test results show that, compared with other methods, the peak load of the line in this paper is smaller and the load curve is smoother, which is conducive to the safe and stable operation of the power grid; it can effectively reduce the loss rate, which is conducive to the economic operation of the power grid, improve the voltage quality, and ensure the power demand of users.

Keywords Internet of things · Intelligent charging control · MPPT algorithm

1 Introduction

The arrival of the Internet of things era brings more convenience for people and more ways to solve some problems. In particular, the energy and environmental problems are becoming more and more serious, which can be controlled and solved in the Internet of things environment. As an indispensable means of transportation in human life, automobile occupies a considerable share in energy consumption and exhaust emissions (Gücin et al. 2019; Babar and Arif 2019). Automobile not only brings convenience to human beings, but also pollutes the environment. The emission of automobile exhaust causes many environmental problems, such as greenhouse effect, destruction of ozone layer, acid rain and so on, which has a great harm to human life. Sharing car is different from fuel car, especially pure sharing car, there is no fuel problem and vehicle exhaust emission problem, so the research and development of sharing car has become a hot spot in the world.

At present, with the promotion of governments all over the world, major global automobile companies are taking active actions to fully prepare for the rapid development of new energy vehicles in the international market. In the future, China's shared cars will usher in a new round of high-speed development, with broad prospects for development. At the same time, domestic major automobile manufacturers have invested unprecedented enthusiasm in the research and development of shared cars. Shared car charging system is an indispensable infrastructure of shared car energy supply after the industrialization of large-scale operation of shared cars. As a new technology field of shared vehicles, it is a weak link in the promotion and application of shared vehicles, which brings great difficulties to the next development and unified planning of shared vehicles. At present, the world-famous automobile enterprises have participated in the research of charging technology, and plan to formulate charging technology standards to lead the future development of enterprises. Therefore, in order to speed up the large-scale industrialization process of shared vehicles, it is urgent to develop advanced, stable, safe and applicable shared vehicle charging system.At present, the research on shared cars in our country mainly focuses on the motor, battery, and other shared cars themselves, and the research

✉ Ling Ma
lumaling@126.com

Ye'an Lu
luyean@126.com

[1] College of Automobile and Rail, Anhui Technical College of Mechanical and Electrical Engineering, Wuhu, China

[2] College of Electrical Engineering, Anhui Technical College of Mechanical and Electrical Engineering, Wuhu, China

Published online: 04 January 2021

on the related subsystem technology of shared cars such as vehicle charging system is relatively less, which seriously hinders the commercial operation of shared cars.

Serious environmental pollution and the reduction of fossil energy accelerate the development of new energy vehicles. As a green travel tool with policy subsidies, the popularity of new energy vehicles is increasing, and the charging behavior is highly uncertain in time and space, resulting in too many shared vehicles without charging arrangement, which brings a series of problems such as load level and power quality improvement to the traditional distribution network, such as the decline of quantity and the increase of network loss. Therefore, the research of power battery is one of the difficulties in the field of shared vehicle research. Power battery charging technology is the core content of all kinds of shared vehicles. In the case of insufficient battery (Zhao et al. 2019), timely and effective supplement of electric energy is very important for shared vehicle range and driving experience. The intelligent charging uses the charging pile fixed on the ground, uses the special charging interface and adopts the conduction mode to provide AC energy for the electric vehicle with on-board charger, which has the corresponding communication, billing and security protection functions. Citizens only need to buy an IC card and recharge it, then they can use the charging pile to charge the car. A good power sharing car needs not only large capacity power battery, but also high-quality charging. High quality charging can not only ensure that the battery is fully charged quickly and efficiently, but also has an important impact on the service life of the battery and the maintenance cost of the battery in the future. It can be seen that the charging technology has played an important role in promoting the development of the car sharing industry.

2 Algorithm definitions

2.1 MPPT basic principle

Solar photovoltaic cells can produce photovoltaic power generation effect in a certain spectral range, but with the change of solar irradiance, its power generation efficiency will change greatly. For a specific solar irradiance, its output characteristics are shown in Fig. 1. In general, MPPT uses search algorithm to track the maximum power point (MPPT), and the position of MPPT can be judged by the electrical signal directly measured (Kathirvel et al. 2016). Including: disturbance observation method: the direction of the maximum power point can be found by continuously disturbing the working point of the solar photovoltaic system. First, the output voltage value is disturbed, and then the power change is measured. Compared with the power before the disturbance, if the power value increases, the disturbance

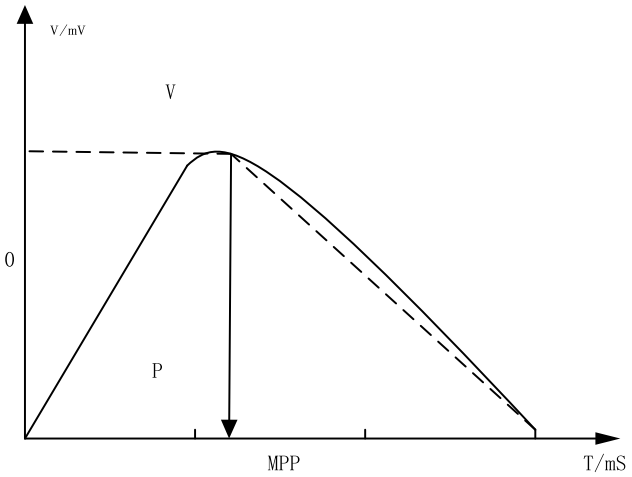

Fig. 1 Output characteristics of photovoltaic cells

direction is correct, otherwise, the disturbance voltage value is reset. It can be seen from the figure that photovoltaic cell is a kind of nonlinear element. When the output current increases, the corresponding output voltage will decrease, and the maximum power point appears in the MPP of Fig. 1.

2.2 MPPT working principle

The working efficiency η of the photovoltaic charger at a certain time is equal to the ratio of the instantaneous power P_b obtained by the battery and the instantaneous output power P_{sp} of the solar panel, as shown in formula 1:

$$\eta = \frac{P_b}{P_{sp}} = \frac{V_b I_b}{V_{sp} I_{sp}} \tag{1}$$

Among them V_{sp} and I_{sp} are the output voltage and current of the solar panel at a certain time, while V_b and I_b are the charging current of the voltage at both ends of the battery. If the battery gets the maximum charging power at a certain time, we can think that the solar panel works at the maximum power point at this time. Due to the characteristics of the battery itself, the voltage at both ends of the battery increases slowly in the process of charging (Zhou et al. 2019), so it can be considered that the voltage at both ends of the battery is unchanged in a short period of time. We can use this characteristic to find the maximum power point of the solar panel. The process can be divided into three steps: first, measure the charging current I_{b1} of the battery at a certain time; second, slightly adjust the duty cycle and change the working point; third, measure the charging current I_{b2} again and compare it with I_{b1}. If $I_{b2}>I_{b1}$, continue to adjust in the just direction; if $I_{b2}<I_{b1}$, adjust in the opposite direction until the maximum power point is found. It is important to note that this process needs to be fast enough to ensure

that the voltage at both ends of the battery remains constant throughout the process.

3 Intelligent charging control method of shared vehicle based on MPPT algorithm

3.1 MPPT algorithm

At present, the commonly used MPPT algorithms mainly include constant voltage tracking method, open circuit voltage proportion method, disturbance observation method, etc. The principle of the open-circuit voltage proportional method is to first collect the output voltage of the photovoltaic cell and make it work at about 80% of the open-circuit voltage, so as to realize the tracking of the maximum power point. Therefore, it is only an approximate maximum power method with obvious disadvantages (Wei-Ya et al. 2013). Disturbance observation method is a commonly used algorithm at present. Its idea is to increase or decrease the output voltage of photovoltaic cell according to a certain time interval, then collect its output current, calculate the output power, and determine whether to increase or decrease the output voltage by comparing with each other. However, this method not only collects the output voltage of photovoltaic cell, but also collects the output current to respond Time is slow, when the external environment changes faster, it fails.

The CVT mode has the advantages of simple control, high reliability and good stability. When the external sunlight intensity changes rapidly, using the Inc mode, its output voltage can stably follow its change, so as to ensure the maximum power output. The control precision is high. Combining the advantages of the two control methods, an improved control algorithm combining the two methods is proposed (Wang et al. 2018). For the boost converter, there are:

$$U_o = \frac{1}{1-D} U_{pv} \tag{2}$$

Among them, U_{pv} express BOOST DC side voltage, that is, the output voltage of photovoltaic panels. Under the condition of U_o stability, the output voltage of photovoltaic cell can be regulated by setting a disturbance U_{oc} and adjusting the duty cycle D, which makes the control more simple and direct. Firstly, the open circuit voltage of the photovoltaic cell is sampled. When the photovoltaic cell operates at the maximum power point, the corresponding relationship between the corresponding output voltage U and the open circuit voltage U_{oc} is as follows:

$$U \approx 0.8 U_{oc} \tag{3}$$

Through the start-up of CVT control system, according to the CVT tracking process, a fixed voltage U_{set} can be set first, its size is close to the voltage value u corresponding to the maximum power point of the photovoltaic cell (if the parameter of U_{oc} is known, make $U_{set} \approx 0.8 U_{oc}$) (Singh et al. 2019). When the system tracks to the maximum power point, the Inc mode is used for precise adjustment. Improved MPPT flow is shown in Fig. 2.

3.2 Load tolerance of charging pile

In order to reduce the damage of overload to the charging grid, load limiting strategy of charging pile is adopted to cut peak. The system takes D as the computing unit and the time interval is 1 min. It is assumed that the maximum load distributed by the power network at Wm in is represented by Pmax, W, namely

$$P_{\max,w} = \sum_{m=1}^{Q} P^{m}{}_{\max,w} w = 1, 2, 3, ..., 1440 \tag{4}$$

$$\text{Among } P^{m}_{\max,w} = P^{m}_{1\max,w} + P^{m}_{0\max,w} + P^{m}_{2\max,w}$$

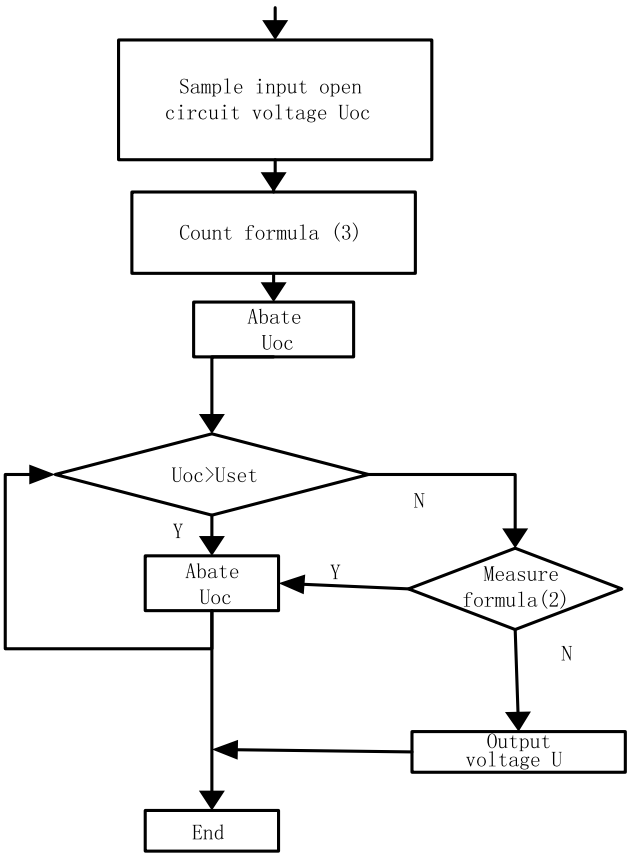

Fig. 2 Improved MPPT flow chart

$$P^{m}_{2\max,w} = \sum_{j=1}^{N} P^{j}_{m\max,w}$$

In formula: Q is the number of regions; $P^{m}_{\max,w}$ is the maximum load provided to area m at W min; $P^{m}_{1\max,w}$ is the maximum load of the user; $P^{m}_{0\max,w}$ is the loss load; $P^{m}_{2\max,w}$ is the maximum charging load; N is the total number of charging piles in M area; $P^{j}_{m\max,w}$ the maximum reserved load allowed for charging point j. The reserved load of each charging point depends on the geographical location, traffic flow and other factors (Shaoqi et al. 2019), the later stage is determined by statistical analysis of computer processing terminal. The power grid control center feeds back with the computer processing terminal according to formula (4), and the computer processing terminal carries out the pre load limit and pre allocation of the charging pile to reduce the damage to the power grid.

3.3 Voltage consumption of precise charging circuit

The running state s of the shared vehicle can be expressed by the vector shown in the following equation, and certain decision-making operations can be carried out through the relevant elements in the system feedback vector.

$$S = \left(E_S, E_B, E_a, D_0, T_S, T_f\right) \tag{5}$$

In formula: E_S initial energy storage for shared vehicles; E_B is the total energy storage; E_a is the average energy consumption; D_0 is the shortest path; T_S is the starting time of charging; T_f is the starting time of charging; The system first judges whether the shared vehicle needs to be charged through the feedback information, and the judgment principle is as follows: According to the average energy consumption E_a, initial energy storage E_S and the minimum allowable residual energy of the shared vehicle, the driving mileage D_R, of the shared vehicle is calculated, km:

$$D_R = \frac{E_S - \partial E_B}{E_a} \tag{6}$$

In formula: ∂ is the limiting factor, which is different for different types of batteries.

Based on the geographic information feedback, the system calculates the shortest travel from the current position to the destination D_1 km and the shortest distance between the destination and the nearest charging station D_2 km, if $D_R > D_1 + D_2$, the shared car does not need to be charged when driving to the destination, otherwise it needs to be charged once. According to the location and destination information of current shared vehicles, all charging points in the range are selected as the main selection set of charging points. Then, the system accountant calculates the shortest path from the current location through the main charging station to the destination D_0 (Masih-Tehrani et al. 2019). Suppose there are m shared cars and N charging piles in total. If the charging pile J is in the primary selection set of shared car I, and the path of shared car I passing through charging pile J to the destination is also in the set D_0, then it is represented by D_0^{ij}:

$$D_0^{ij} = D_0^{ij}(1) + D_0^{ij}(2) \tag{7}$$

Among them $i = 1, 2, 3, 4, ..., M$, $j = 1, 2, 3, 4, ..., N$.

In formula: The distance from shared vehicle i to charging point j; is the distance from charging point j to the destination. After submitting the appointment, the starting time of charging of shared vehicle i at charging point j is as follows:

$$D_0^{ij}(1)D_0^{ij}(2)T_S^{ij} = T_0^{i} + t_1^{ij} + t_2^{ij} \cdots \tag{8}$$

In formula: T_0^i is the appointment time of sharing car i; t_1^{ij},t_2^{ij} ,…, is the driving prediction time from shared vehicle i to charging point j. Since the change of traffic volume will cause the change of charging time, according to the real-time road condition information, the time is calculated once every several minutes, real time prediction of the start time T of shared vehicle i charging

$$T_{SI}^{ij} = T_0^{i} + t_1^{ij} + t_2^{ij} \cdots \tag{9}$$

In formula: t_1^{ij}, t_2^{ij},…, they are the time of passing each road section predicted in combination with traffic conditions.

Through the comparative calculation of $T_{SI}^{ij} - T_0^{k}$, the charging sequence numbers of shared vehicle i and shared vehicle k are adjusted. Among them, the shared vehicle i and the shared vehicle k both submit an appointment for the charging post j and i ≠ k. The charging time of shared vehicle i at charging point j is expressed by t_d^{ij}. According to the average energy consumption E_a^i, initial energy storage E_S^i, reserve state E_B^i and total energy storage ϑ of the shared vehicle i, the remaining electricity quantity arriving at the charging post j is calculated (Liu 2019), according to the charging power of P_C^j charging post, the charging time is calculated as follows:

$$t_d^{ij} = \frac{\vartheta E_B^i - \left[E_S^i - E_a^i D_0^{ij}(1)\right]}{P_C^j} \tag{10}$$

Due to the fact that some users consider more to replenish the power as soon as possible rather than to fully charge the battery, considering the two factors of prolonging the battery life and shortening the charging time, according to the urgency of users, the reserve status at the end of the time ϑ is set to be 75%, 80% and 85%. Calculation shared car i leave the charging station j moment t_f^{ij} satisfaction:

$$t_f^{ij} = T_S^i + t_P^{ij} + t_d^{ij} \tag{11}$$

In formula: t_P^{ij} is the queuing time of shared vehicle i at charging station j, as follows:

$$t_P^{ij} = \sum_{h=1}^{H} \left[\left(T_f^{hj} - T_s^{hj} \right) + t_h^j \right] \tag{12}$$

In formula: t_h^j is the other consumption time of the h shared car in the charging station, determined according to the general time consumption of statistical models (Liu et al. 2019), $h \neq i \in H$; H∈M is the total number of shared cars booked up to the i shared car.

Real time prediction of shared cars i leave the charging station j moment T_{ft}^{ij} satisfaction:

$$T_{ft}^{ij} = T_{SI}^{ij} + t_{pl}^{ij} + t_d^{ij} \tag{13}$$

Shared car i appointment charging post j ,initial predicted consumption time from appointment to completion of charging time T_1^{ij} can be expressed as

$$T_1^{ij} = T_f^{ij} - T_0^{ij} \tag{14}$$

In formula: T_0^{ij} is the starting time for sharing car i to reserve charging point j. The real-time prediction consumption time is as follows:

$$T_{1l}^{ij} = T_{fl}^{ij} - T_0^{ij} \tag{15}$$

For cost Y^{ij} (including charging cost and road consumption cost) yuan, it can be expressed as follows:

$$Y^{ij} \left\{ \vartheta E_B^i - \left[E_S^i - E_a^i D_0^{ij}(1) \right] \right\} C_j + E_a^i D_0^{ij} C_0 \tag{16}$$

In formula: C_j is the regulated electricity price of charging pile j, used to adjust the charging distribution of users; C_0 is the standard price. By solving the above model, computer network terminal can provide users with three selection strategies (Liu et al. 2018), as follows:

$$\begin{cases} T_f^{ij} = \min\left\{ T_f^{ij} \right\} \\ Y^{ip} = \min\left\{ Y^{ij} \right\} \\ R^{jr} = \min\left\{ cT_f^{ij} + bY^{iJ} \right\} \end{cases} \tag{17}$$

where, c is the weight coefficient, and B is the ratio between decision cost and time. According to Eq. (17), the matching set of charging piles can be obtained. Charging point Q has the shortest charging time, charging point P has the lowest charging cost, and charging pile R is the best, so as to meet charging demands of different intentions.

4 Experimental study

In order to evaluate the effectiveness of the MPPT based intelligent charging control method for utility vehicles in the Internet of things environment, this paper studies the steady-state impact of charging utility vehicles on medium and low-voltage distribution network by using Google Analytics platform, and compares with other charging strategies (Boukens et al. 2018).

The method to evaluate the impact of different charging strategies on distribution network is as follows: according to the determined scheme, the shared vehicles are allocated to each bus of the network, and the daily load of the shared vehicles is determined. Three charging strategies, namely disorder charging, time of use charging and intelligent charging, are used to evaluate the impact of shared vehicles on distribution network. Time sharing price is a simple peak and valley price. Taking a large province in Southeast China as an example, it is divided into peak period 8:00–22:00 and the next day's low period 22:00–8:00.

It is assumed that the inherent charging load of the shared vehicle will appear in each node of the grid (Cai et al. 2019), and it is directly proportional to the installed capacity of the residential power of each node. When different charging strategies are implemented, this method can estimate the maximum number of shared vehicles that a given distribution network can safely carry. In order to facilitate the calculation, it is assumed that the shared car battery is always charged at a constant power of 3 km, and sharing a car for 4 h a day, namely $p_{ev} = 3, T = 4$, then each shared car absorbs 12 km·h of electric energy from the grid every day. Assuming that the electric energy consumed per kilometer is 0.2 km·h, the electric energy absorbed every day can make the shared car drive 60 km at a time.

4.1 Experimental steps

4.1.1 Determine the time when the shared vehicle is connected to the grid

Suppose that the shared car only drives twice a day, and each charging time is between the end of the last driving of the previous day and the first driving of the next day. The travel time probability distribution shown in Fig. 3 is obtained by using the statistical method to study the characteristics of common traffic behavior of shared cars in a certain area. There is no big difference between the driving habits of car sharing users and ordinary private cars, so it is assumed that the driving rules of shared car users are similar. The probability distribution of daily travel time

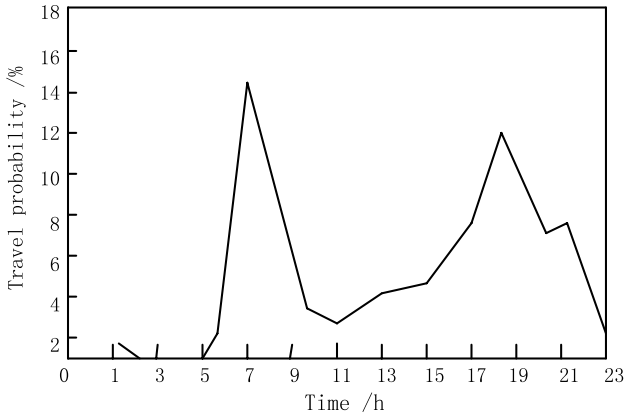

Fig. 3 Probability distribution of daily travel time of shared vehicles

shown in the figure is based on Wang zuozhi's travel probability statistics (Cheng et al. 2019). Since the charging time of each shared vehicle is assumed to be 4 h, the time interval between the last driving end of the previous day and the first driving start of the next day must be at least 4 h.

4.1.2 Determine the effective energy absorption time of shared vehicles from the grid

When using unordered charging, assume that the owner will connect the Shared car to charge at any time. As a result, when the owner goes home, the car will automatically start charging for 4 h after it is connected. When the time-sharing tariff is adopted, it is assumed that under the guidance of tariff, the owners of shared cars will charge when the tariff is low, that is to say, the electric vehicles will be charged between 22:00 and 8:00. Only when the access time is less than 4 h during the low price period, the shared car will be charged outside this time. As for intelligent charging, it can be determined by solving the integer programming problem of Eqs. (15)–(17) (Armaghani et al. 2019).

4.1.3 Determine the distribution of shared vehicles

After the charging time of the shared vehicle is determined, the above charging strategy is studied. Considering that the installed capacity of the shared load vehicle is proportional to the normal load of each bus, the calculation method of formula (18) is that the number of shared vehicle buses connected to each grid is as follows:

$$N_{ev,j} = \frac{L_{Rj}}{\sum_{j=1}^{m} L_{Rj}} \times n, j \in [1, m] \tag{18}$$

In formula: $N_{ev,j}$ is the number of shared vehicles connected to bus y;L_{Rj} is the residential load installed on bus y(kW); $\sum_{j=1}^{m} L_{Rj}$ is the total residential power load in the network(kW).

The result of Eq. (18) will make the bus with high residential load distribute more shared cars. According to the conclusion of formula (18), all shared vehicles will have corresponding bus number, that is, the bus to which they are connected for charging (Pare et al. 2017). This process can calculate the shared vehicle load of each node of the system in each time step.

4.1.4 Determine the daily load after the shared vehicle is connected

Finally, add each EV load to the conventional load, and calculate the total load and load of the power grid under the three charging strategies. The calculation formula is as follows:

$$L_{Tj}^{t} = L_{t}^{j} + \sum_{k=1}^{N_{evj}} C_{t}^{k} \times P_{ev}, \begin{cases} j \in [1, m] \\ k \in \left[1, N_{ev,j}\right] \\ t \in [1, 24] \end{cases} \tag{19}$$

In formula: L_{Tj}^{t} is the total load of bus y in the R period (kw); C_{t}^{k} is the state of charge vector of the kth shared vehicle (composed of 24 binary variables). If $C_{t}^{k} = l$, indicates that the a shared vehicle is charged in the t time period; if $C_{t}^{k} = 0$, indicates that the fourth shared vehicle does not charge in the t time period. K is the shared vehicle label assigned to bus y.

4.2 Experimental result

In the experiment, the following three situations are considered: all shared vehicles adopt disordered charging strategy, all shared vehicles adopt time-sharing pricing charging strategy, and all shared vehicles adopt intelligent charging strategy, and the maximum number of shared vehicles that can be safely accessed in the network is evaluated. The maximum allowable access amount of shared vehicles is gradually increased until the voltage exceeds the line or a branch overload occurs.Then the influence of shared vehicle charging on a suburban medium voltage power grid is evaluated by the above algorithm. It is assumed that the shared vehicle charging load is connected to each grid node and is proportional to the installed residential load of the node. The analysis objects in the simulation include the change of load curve, voltage distribution and power loss.

The typical 15 kV suburban medium voltage distribution network shown in Fig. 4 is taken as the experimental

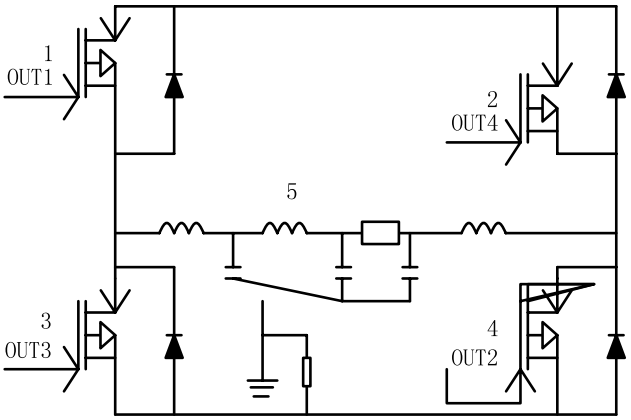

Fig. 4 Suburban medium voltage distribution network

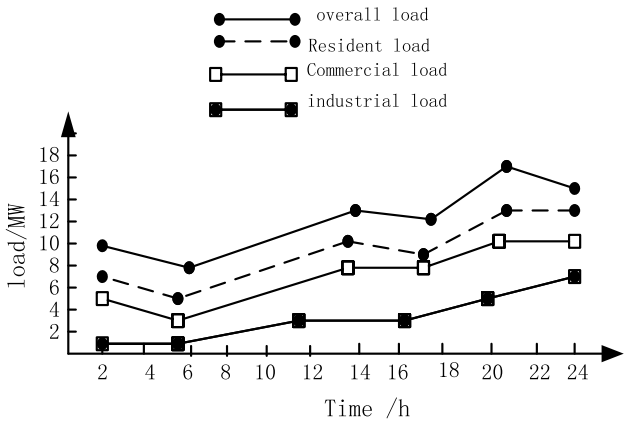

Fig. 5 Typical daily load curve

case of this study. The numbers 1–5 in the figure indicate the buses that are prone to voltage problems, and the normally open branches are represented by dotted lines, including two power supply points, which are represented by circles in the figure. At the power supply point, the given voltage is 1.05p. U, and the power factor of conventional load is assumed to be 0.96.

Typical daily load curve of medium-voltage distribution network is shown in Fig. 5. Among them, residential load accounted for 66%, commercial load accounted for 28%, industrial load accounted for 6%. The ratio is proportional to the installed capacity of each load. The power of the selected typical daily peak load is 16.6 MW, and the power consumption is about 277 MW · H-1. Assuming that each household has an average of 1.5 Shared cars, it can be determined that the total number of Shared cars in the geographic area of the grid is about 127,000. The simulation results are as follows.

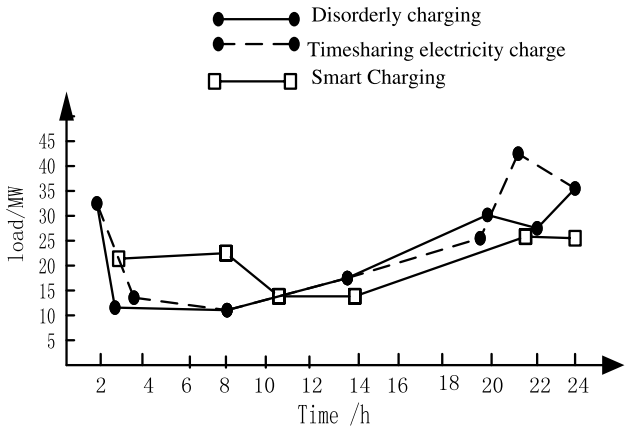

Fig. 6 Load curve with 63% access ratio of shared vehicles ®

Table 1 Voltage on bus 1–5 (P.U)

Generatrix	1	2	3	4	5
No electric cars	0.961	0.962	0.962	0.962	0.964
Disorderly charging	0.843	0.844	0.847	0.851	0.858
Timesharing electricity charge	0.833	0.835	0.835	0.837	0.838
Smart charging	0.902	0.902	0.904	0.905	0.905

4.2.1 Maximum allowable access consumption of shared vehicle

In the medium voltage power grid, the maximum allowable access proportion of shared vehicles is 17% for disordered charging strategy, 20% for time-sharing pricing strategy and 63% for intelligent charging strategy. Such a proportion of the number of shared vehicles is based on the total number of conventional vehicles within the geographical scope of the grid. Therefore, for disordered charging strategy, time-sharing pricing charging strategy and intelligent charging strategy, the number of shared vehicles that the grid can safely access is 2159, 2540 and 8001, respectively.

4.2.2 Change of load curve

The load curve shown in Fig. 6 is the load curve under different charging strategies. It is assumed that the access proportion of shared vehicles is 63%, that is, the maximum possible access proportion of shared vehicles under intelligent charging strategy without strengthening the power grid. The peak load of power grid is 16.6 mw without common load. The peak load is increased to 34.4 MW with disordered charging strategy, increase to 36.6 MW in time of use tariff charging strategy, Smart charging strategy increased to 20.8 MW. Obviously, the intelligent charging strategy has a better effect of reducing peak load, because when the access

ratio of shared cars is 63%, corresponding to the access of about 8000 shared cars, the peak load only increased by 4.2 MW.

4.2.3 Voltage distribution

As shown in Table 1, according to the data, the impact of shared vehicle access on the voltage distribution of some buses far away from the power supply point in electrical distance can be evaluated. The data in the table adopts the standard value.

The voltage drop of five buses is the largest. For the disordered charging strategy, the average voltage drop of the five most critical buses is 11.8%, and the bus 1 farthest from the power supply bus has the largest voltage drop. The average voltage drop of the five buses is 13.2% when the timesharing charging strategy is used. The intelligent charging strategy can obtain better voltage distribution. When using this charging strategy, although the voltage of these buses drops by 6.1% on average, it is not lower than the lower limit value of voltage: 0.90 p. U.

It can be seen from Table 1 that for bus 1 with the largest voltage drop, the voltage drop under the three charging strategies is 12.3%, 13.3% and 6.1%, respectively, which is close to the lower voltage limit when adopting the intelligent charging strategy. For this reason, 63% of the shared vehicle access ratio represents the maximum possible limit value under the intelligent charging strategy, because for a higher access level, the voltage will be lower than 0.90 p.U. Similarly, for the unordered charging strategy and time-sharing pricing charging strategy, when the voltage reaches the lower limit, the access consumption rate of the sharing car is 17% and 20%, respectively. The voltage of the most serious bus 1 under different charging strategies is analyzed. The results show that the voltage is the factor limiting the high access of the Shared vehicle. Compared with the maximum load limit of the branch, the lower limit of the voltage is reached first under the same access rejection ratio. Better results can always be achieved by adopting an intelligent charging strategy (Gao et al. 2020).

4.2.4 Power loss

The daily power loss under the three charging strategies is shown in Fig. 7. The bars represent the absolute value of power consumption, while the small squares represent their proportion of total power consumption. As expected, the smart charging strategy works better because it optimizes load distribution throughout the day and reduces peak load. In the calculation of power loss, its value is directly proportional to the quadratic power of current, while the current is very large in peak load period, so peak load period is the most critical for power loss. The optimization results

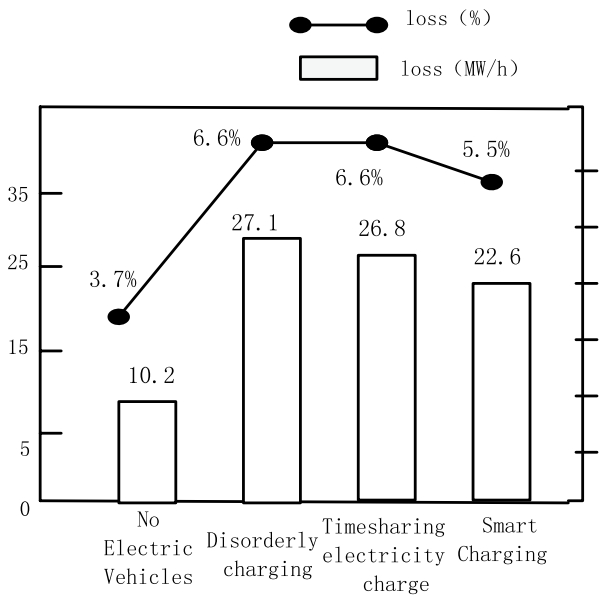

Fig. 7 Daily power loss under three charging strategies

are shown in Fig. 7. The intelligent charging strategy has a smaller peak load, and the strategy of power loss calculation results will achieve the goal of reducing loss and energy saving than the other two charging strategies, so as to realize the optimal economic operation of the power grid, so as to avoid a large amount of investment. It is necessary to strengthen the network construction and improve the economic benefits.

5 Discussion

This paper summarizes several main charging strategies, and then puts forward an intelligent charging control method based on MPPT algorithm in the Internet of things environment. The control structure can aggregate certain scale electric vehicle users in the region and participate in the power control management. The intelligent charging path with the minimum peak load of power grid as the optimization objective is established, and the method to evaluate the influence of electric vehicle charging on the distribution network under different charging strategies is evaluated.

The charging load of electric vehicle is determined by determining the location and time when the electric vehicle is connected to the power grid, and the specific steps and algorithm flow are formulated. Three charging strategies are used to evaluate the influence of EV charging on a medium voltage power grid. The results show that the intelligent charging strategy can effectively reduce the peak load of the charging load, obtain better voltage distribution and lower power loss, and is more conducive to the safe and stable and economic operation of the power grid, which is an ideal

charging optimization control strategy. The experimental results show that the peak load of the line is small and the load curve is smooth, which is conducive to the safe and stable operation of the power grid. It can effectively reduce the network loss rate, is conducive to the economic operation of the power grid, improve the voltage quality, and ensure the demand of users.

6 Conclusion

Electric vehicle charging control is an important part of power grid load management. Through appropriate charging control, especially the intelligent charging control method based on MPPT algorithm in the Internet of things environment, it can not only effectively control the negative impact of charging load on the electric system, but also enrich the operation and control means of the system, track the renewable energy output, and generate huge benefits. For example, the charging control of electric vehicles can achieve peak cutting and valley filling, and support the power grid Operation, play the role of load dispatching, make the peak load of the line smaller, load curve more smooth, conducive to the safe and stable operation of the grid;It can effectively reduce the power loss rate, help the economic operation of the power grid, improve the voltage quality, so as to ensure the power demand of users. Therefore, it is of great theoretical and practical significance to study the charging control of electric vehicles in distribution network and adopt effective scheduling strategies.

Acknowledgements The research is supported by A Key Project of Higher Education Natural Science Foundation of Anhui Province of China: research on design methods of automotive products based on user needs and enterprise preferences (Grant No. KJ2019A1161).

References

Armaghani DJ, Koopialipoor M, Marto A, Yagiz S (2019) Application of several optimization techniques for estimating TBM advance rate in granitic rocks. J Rock Mech Geotech Eng 11(4):779–789

Babar M, Arif F (2019) Real-time data processing scheme using big data analytics in internet of things based smart transportation environment. J Ambient Intell Humaniz Comput 10(10):4167–4177

Boukens M, Boukabou A, Chadli M (2018) A real time self-tuning motion controller for mobile robot systems. IEEE/CAA J Automatica Sinica 6(1):84–96

Cai L, Hu P, Tan Z (2019) Research on the effect of large-scale electric vehicle based on smart wearable equipment access to grid. J Ambient Intell Humaniz Comput 10(8):3231–3237

Cheng J, Jiang CHEN, Xiang H (2019) A surface parametric control and global optimization method for axial flow compressor blades. Chin J Aeronaut 32(7):1618–1634

Gao W, Senel M, Yel G, Baskonus HM, Senel B (2020) New complex wave patterns to the electrical transmission line model arising in network system. AIMS Math 5(3):1881–1892

Gücin TN, Biberoğlu M, Fincan B (2019) Constant frequency operation of parallel resonant converter for constant-current constant-voltage battery charger applications. J Modern Power Syst Clean Energy 7(1):186–199

Kathirvel C, Gopinath M, Porkumaran K, Jagannathan S (2016) Design and simulation of an advance rectifier stage topology with MPPT for hybrid energy system. Asian J Inf Technol 15(1):162–168

Liu F, Chen K, Zhao Z, Li K (2018) Analysis of transmitter-side control methods in wireless EV charging systems. Sci China Technol Sci 61(10):1492–1501

Liu B (2019) System deployment and decentralized control of islanded AC microgrids without communication facility. J Modern Power Syst Clean Energy 7(4):913–922

Liu YK, Zhang XS, Zhang L, Tao F, Wang LH (2019) A multi-intelligence architecture for platform-based intelligent manufacturing system scheduling. Front Inf Technol Electron Eng 20(11):1465–1493

Masih-Tehrani M, Yazdi MRHI, Esfahanian V, Dahmardeh M, Nehzati H (2019) Wavelet-based power management for hybrid energy storage system. J Modern Power Syst Clean Energy 7(4):779–790

Pare S, Kumar A, Bajaj V, Singh GK (2017) A context sensitive multilevel thresholding using swarm based algorithms. IEEE/CAA J Automatica Sinica 6(6):1471–1486

Shaoqi WANG, Dongli MA, Muqing YANG, Zhang L, Guanxiong LI (2019) Flight strategy optimization for high-altitude long-endurance solar-powered aircraft based on Gauss pseudo-spectral method. Chin J Aeronaut 32(10):2286–2298

Singh KV, Bansal HO, Singh D (2019) A comprehensive review on hybrid electric vehicles: architectures and components. J Modern Transport 27(2):77–107

Wang Z, Diao Y, Zhao Y, Liang L, Wang T (2018) Experimental study on the new type of electrical storage heater based on flat micro-heat pipe arrays. Sci China Technol Sci 61(2):219–231

Wei-Ya Z, Yong-Li L, Xiao-Yong C, Nan W (2013) Dynamical investigation and parameter stability region analysis of a flywheel energy storage system in charging mode. Chin Phys B 22(9):619–632

Zhao K, Wang Y, Han L, Wang Y, Luo X, Zhang Z, Yang Y (2019) Nanogenerator-based self-charging energy storage devices. Nano-Micro Lett 11(1):1–19

Zhou Z, Zhang L, Liu Z, Ma L, Huang M, Su H (2019) Design and demonstration of a dynamic wireless power transfer system for electric vehicles. Sci China Inf Sci 62(12):223–241